Materials Science and Engineering B 167 (2010) 70–73

Contents lists available at ScienceDirect

Materials Science and Engineering B

journal homepage: www.elsevier.com/locate/mseb

Short communication

Influence of annealing temperature on surface morphology and magnetic properties of $Ni_{0.7}Zn_{0.3}Fe_2O_4$ ferrite thin films

Zhenfa Zi[a,b], Hechang Lei[a], Xiangde Zhu[a], Bo Wang[a], Shoubao Zhang[a], Xuebin Zhu[a], Wenhai Song[a], Yuping Sun[a,c,*]

[a] Key Laboratory of Materials Physics, Institute of Solid State Physics, Chinese Academy of Sciences, Hefei 230031, People's Republic of China
[b] Department of Physics and Electronic Engineering, Hefei Normal University, Hefei 230061, People's Republic of China
[c] High Magnetic Field Laboratory, Chinese Academy of Sciences, Hefei 230031, People's Republic of China

ARTICLE INFO

Article history:
Received 11 April 2009
Received in revised form
15 November 2009
Accepted 17 January 2010

Keywords:
$Ni_{0.7}Zn_{0.3}Fe_2O_4$ ferrite films
Chemical solution deposition
Coercivity

ABSTRACT

Nickel–zinc (Ni–Zn) ferrite $Ni_{0.7}Zn_{0.3}Fe_2O_4$ thin films were fabricated on Si(0 0 1) substrate by a simple chemical method. The microstructure and magnetic properties were systematically investigated. X-ray diffraction results show that all samples have a single-phase spinel structure with the space group of $Fd\bar{3}m$. The results of field-emission scanning electronic microscopy show that the mean grain size increases from 10 to 32 nm with increasing the annealing temperature from 500 to 900 °C. The magnetic properties of $Ni_{0.7}Zn_{0.3}Fe_2O_4$ ferrite thin films exhibit a strong dependence on the annealing temperature. The coercivity increases from 25 to 80 Oe and the saturation magnetization increases from 146 to 283 emu/cm^3 with increasing the annealing temperature, which is in favor of modern electronic device miniaturization.

1. Introduction

In the past decades, nickel–zinc (Ni–Zn) ferrites have been widely used as high-performance microwave devices due to their high resistivity, high Curie temperature, strong mechanical hardness, excellent soft magnetic properties at high frequency, and chemical stability [1–4]. Ni–Zn ferrite is a type of mixed spinel in which tetrahedral (A) sites are occupied by Zn^{2+} and Fe^{3+} ions, whereas the octahedral (B) sites are occupied by Ni^{2+} and Fe^{3+} in the cubic spinel lattice. These two antiparallel sublattices form a ferrimagnetic structure, in which $Ni^{2+}$and $Fe^{3+}$are coupled by superexchange interactions through the O^{2-} ions.

At present, bulk Ni–Zn ferrite components employed in discrete devices at microwave frequencies are not compatible with the rapid developments of electronic applications towards miniaturation, high density, integration, and multifunction. Thus, more attention has been attracted to solve these difficulties in performing the required miniaturization for complex devices [5]. Ni–Zn ferrite films may play an important role in facilitating the design and fabrication of devices such as micro-inductors, micro-transformers, and microwave nonreciprocal devices [6]. The ferrite thin films incorporated into magnetic integrated circuits are expected to replace the current surface mounting modules in the near future.

The successful growth of magnetic Ni–Zn ferrite films is an important step towards their future incorporation as inductors and transformers into integrated circuits operating at high frequency. Several Attempts have been made by researchers to deposit Ni–Zn ferrite films by a variety of techniques including alternative sputtering technology [7], pulsed-laser deposition [8], and spin-spray plating [9]. However, most of them cannot be economically applied on a large scale because they require high vacuum system, complicated experimental steps, and high reaction temperatures. Additionally, the higher coercivity in Ni–Zn ferrite films compared with bulk materials, which leads mainly to eddy current loss, has become a barrier in the way of applications.

In this study, the chemical solution deposition (CSD) was applied to synthesize $Ni_{0.7}Zn_{0.3}Fe_2O_4$ ferrite thin films on Si(1 0 0) substrates. As a result, the annealing temperature for the crystallization is comparatively low (500 °C) as to obtain homogeneous films with small grain size, and the coercivity of Ni–Zn ferrite films is also low, which are required for fabrication of devices. Using CSD method is useful to achieve the low-temperature fabrication of magnetic ferrite films, which is an efficient way to fabricate integrated thin film devices. The composition $Ni_{0.7}Zn_{0.3}Fe_2O_4$ was selected because its magnetic properties are superior to those of other composition in $Ni_xZn_{1-x}Fe_2O_4$ ($0 \le x \le 1$) system in previous report [10].

* Corresponding author at: Key Laboratory of Materials Sciences, Institute of Solid State Physics, Chinese Academy of Sciences, Hefei 230031, People's Republic of China. Tel.: +86 551 5592757; fax: +86 551 5591434.
E-mail addresses: zfzi@issp.ac.cn (Z. Zi), ypsun@issp.ac.cn (Y. Sun).

0921-5107/$ – see front matter © 2010 Elsevier B.V. All rights reserved.
doi:10.1016/j.mseb.2010.01.033

2. Experimental procedure

Ni–Zn ferrite $Ni_{0.7}Zn_{0.3}Fe_2O_4$ films were prepared by the CSD method. The starting materials were high-purity nickel nitrate hexahydrate $Ni(NO_3)_2{\cdot}6H_2O$, zinc nitrate hexahydrate $Zn(NO_3)_2{\cdot}6H_2O$, and ferric citrate pentahydrate $FeC_6H_5O_7{\cdot}5H_2O$. The starting materials were dissolved in a mixture of ethylene glycol and 2-methoxyethanol at 70 °C and stirred at this temperature for 30 min. The transparent solution with brown color was shaken in ultrasonic cleaner 20 min and stirred at room temperature for 20 h in order to get a well-mixed solution. The total concentration of the metal ions was 0.2 M. The films were prepared by spin-coating method on Si(1 0 0) substrates using rotation speed of 4000 rpm and time of 50 s, and then the as-deposited films were baked at 300 °C for 30 min in order to expel out the organics. The spinning-coating and dry procedures were repeated for four times in order to obtain films with desired thickness. The dried films were annealed at selected temperatures varying from 500 to 900 °C in the air for 20 min in order to get crystallized films.

The crystal structure was examined by Philips X'pert PRO X-ray diffractometer (XRD) with Cu Kα radiation at room temperature. Field-emission scanning electronic microscopy (FE-SEM, FEI designed Sirion 200 type) was carried out to check the morphology and thickness. Surface root-mean roughness was estimated by atomic force microscope (AFM Park Scientific Instruments designed, Autoprobe CP type). Magnetic measurements were conducted with a SQUID magnetometer (MPMS, Quantum design).

3. Results and discussion

The room temperature XRD patterns of $Ni_{0.7}Zn_{0.3}Fe_2O_4$ ferrite thin films annealed at different temperatures are shown in Fig. 1. All of peaks can be indexed to a single-phase spinel structure with the space group of $Fd\bar{3}m$. With increasing the annealing temperature, the relative intensity of the peak (1 1 3) enhances gradually while the full width at half-maximum (FWHM) of the peak (1 1 3) reduces. This indicates $Ni_{0.7}Zn_{0.3}Fe_2O_4$ ferrite grains grow larger and larger with increasing the annealing temperature. According to the low angle (1 1 3) peak central positions, the ferrite lattice parameter was estimated to be 8.362 ± 0.002 Å.

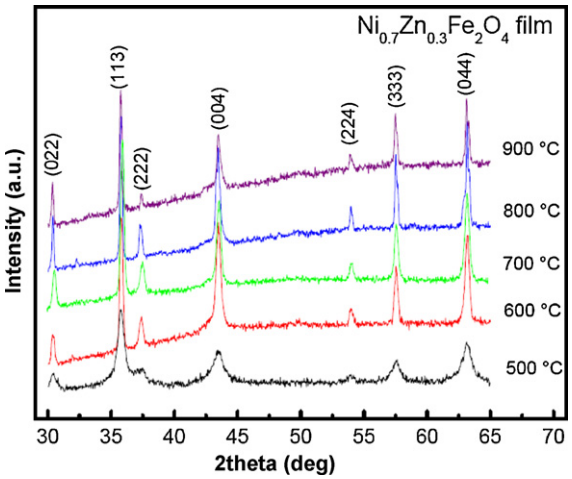

Fig. 1. XRD results of the $Ni_{0.7}Zn_{0.3}Fe_2O_4$ ferrite films on Si(1 0 0) substrates annealed at different temperatures from 500 to 900 °C.

Fig. 2(A)–(E) shows the FE-SEM results for different $Ni_{0.7}Zn_{0.3}Fe_2O_4$ films annealed at different temperatures. It is clearly seen that the grain size increases with increasing the annealing temperature. The mean grain size is 10, 15, 18, 23, and 32 nm for the films annealed at 500, 600, 700, 800, and 900 °C, respectively. Moreover, it is seen that the grain size are rather homogenous. Fig. 2(F) shows the cross-sectional SEM result of the film annealed at 500 °C. It can be seen that the thicknesses of the film is about 200 nm. Additionally, it is observed that the film thickness is independent of the annealing temperature.

The surface morphologies of the $Ni_{0.7}Zn_{0.3}Fe_2O_4$ films have been characterized by AFM. The typical image is shown in Fig. 3(A) for the sample annealed temperature 800 °C, which reveals a rather smooth surface. The surface roughness is in the root-mean square (RMS) range from 1.5 to 4.5 nm. The result of the surface rough-

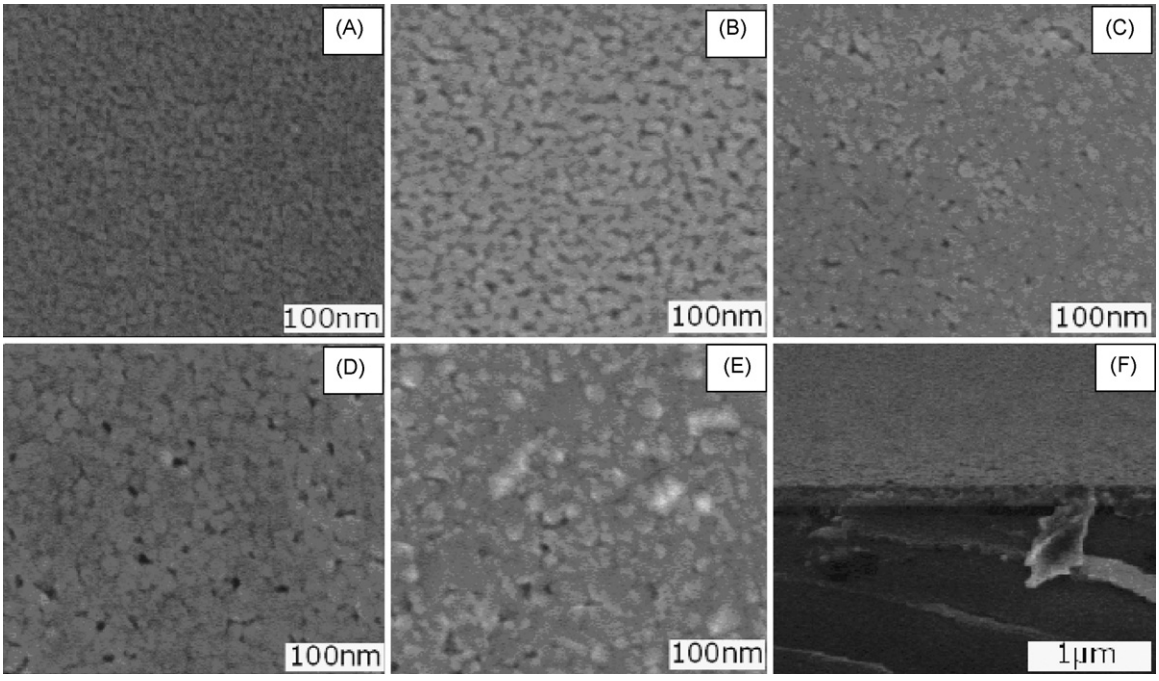

Fig. 2. FE-SEM micrographs of $Ni_{0.7}Zn_{0.3}Fe_2O_4$ ferrite films annealed at different temperatures: (A) 500 °C, (B) 600 °C, (C) 700 °C, (D) 800 °C, (E) 900 °C, and (F) is the cross-sectional SEM micrographs of films annealed at 500 °C.

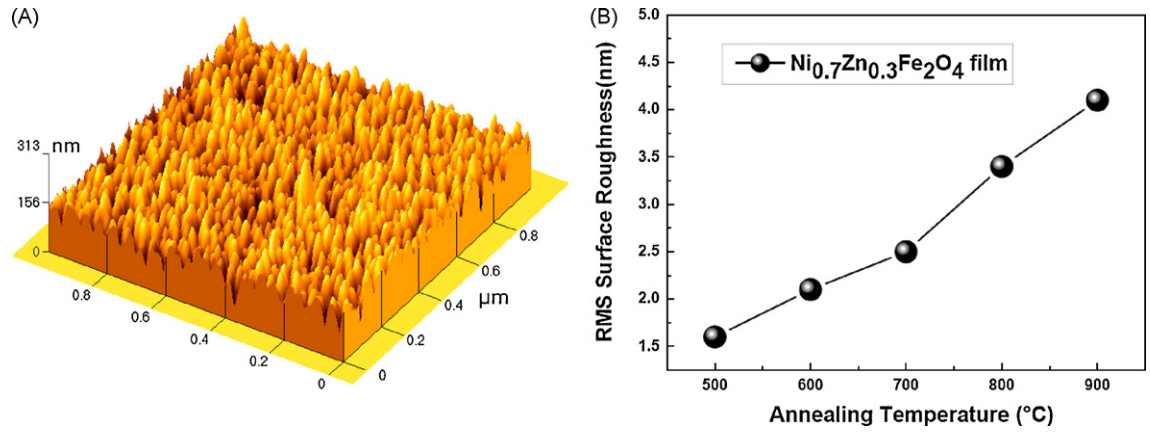

Fig. 3. (A) AFM image of $Ni_{0.7}Zn_{0.3}Fe_2O_4$ ferrite film surface annealed at 800 °C and (B) the dependence of surface roughness on annealing temperatures.

ness is shown in Fig. 3(B) as a function of annealing temperature. The surface roughness is strongly dependent on the annealing temperature. That is, the surface roughness linearly increases with the annealing temperature. When the annealing temperature increases, $Ni_{0.7}Zn_{0.3}Fe_2O_4$ ferrite grains with higher energy have enough mobility on the thermal substrate. Larger $Ni_{0.7}Zn_{0.3}Fe_2O_4$ grains can enhance the surface roughness. The mean grain size estimated through Image Processing in PSI ProScan software from AFM image of the $Ni_{0.7}Zn_{0.3}Fe_2O_4$ film annealed at 800 °C is about 28 nm, which is slightly larger than that estimated from FE-SEM micrographs.

The M (H) loops at 300 K under external fields from −20 to 20 kOe, which are parallel to the film plane, are shown in Fig. 4. It is seen that all $Ni_{0.7}Zn_{0.3}Fe_2O_4$ ferrite films exhibit hysteresis behavior in the M (H) curves, indicating the characteristic of ferrimagnetism, which confirms the desired Ni–Zn ferrite films were successfully obtained.

Fig. 5(A) presents the annealing temperature dependence of the coercivity (H_c). The value of H_c refers to the strength of the magnetic field required to reduce the magnetization of the magnetic sample to zero, after the saturation magnetization of the sample has been reached. It is found that the H_c is enhanced with the increasing annealing temperature. To understand H_c mechanism clearly, the critical size of a monodomain particle can be estimated by the following formula [11]:

$$D_m = \frac{9\sigma_w}{2\pi M_s^2} \quad (1)$$

where $\sigma_w = (2k_BT_C|K_1|/a)^{1/2}$, $|K_1|$, T_C, M_s, k_B, a are the wall density energy, magnetocrystalline anisotropy constant, Curie temperature, Boltzmann constant and, lattice constant, respectively. For $Ni_{0.7}Zn_{0.3}Fe_2O_4$ ferrite, $M_s = 270$ Gs, $T_C = 860$ K, $a = 8.345 \times 10^{-8}$ cm, and $|K_1| = 6.5 \times 10^4$ erg/cm^3 [12], which give the value of D_m ~72.9 nm. The calculated value is larger than that of our sample. Therefore, our samples should exhibit the monodomain behavior. According to Herzer's random anisotropy model [13], the grain size has a large influence on H_c, that is, H_c decreases with a decrease in grain size. This can be understood by the fact that as the domain contains many grains, the magnetocrystalline anisotropy is averaged over many grains and various orientations. The reduced anisotropy leads to a decrease in coercivity with decreasing grain sizes.

Fig. 5(B) exhibits the dependence of the saturation magnetization on the annealing temperature (M_s) with the applied fields paralleling to the film surfaces. It is seen that M_s exhibits an increasing tendency with increasing the annealing temperature. The enhancement in magnetization can be attributed to the improvement of the crystallinity during annealing processing, leading to

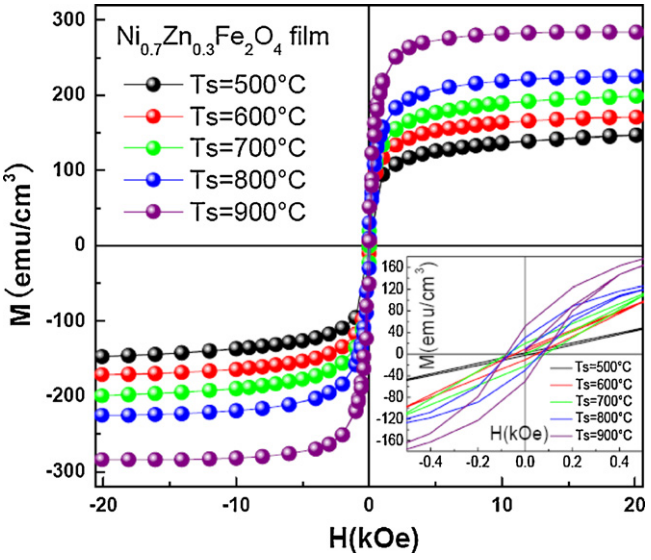

Fig. 4. Room temperature M (H) hysteresis loops of the $Ni_{0.7}Zn_{0.3}Fe_2O_4$ ferrite thin films annealed at different temperatures. The inset contains the minor loops.

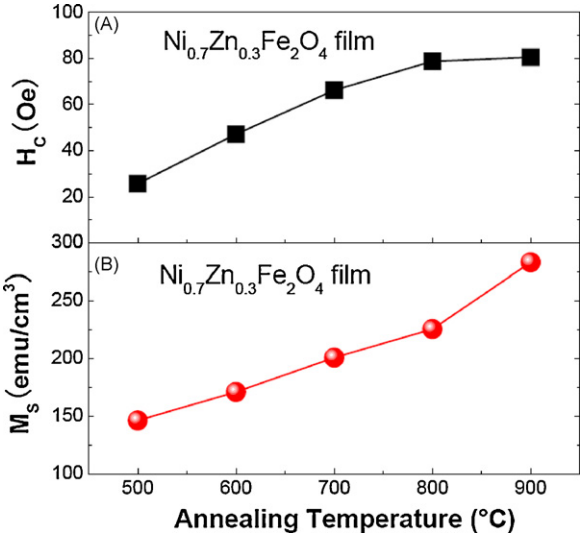

Fig. 5. (A) The coercivity H_c as functions of annealing temperature of the $Ni_{0.7}Zn_{0.3}Fe_2O_4$ ferrite thin films and (B) the dependence of the saturation magnetization M_s on annealing temperature.

the change in degree of inversion parameter due to the increase in grain size [14,15], and the decreased spin disorder in the shell [16].

4. Conclusions

In conclusion, the CSD method was used to prepare $Ni_{0.7}Zn_{0.3}Fe_2O_4$ ferrite thin films. The effects of annealing temperature on the microstructure as well as the magnetic properties were investigated. The FE-SEM results showed that uniform $Ni_{0.7}Zn_{0.3}Fe_2O_4$ films with thicknesses of 200 nm can be obtained, while the grain size increases with increasing the annealing temperature. The excellent magnetic properties including room temperature M_s and H_c indicate the Ni–Zn ferrite films can be considered as a potential candidate for modern miniaturization of electronic devices.

Acknowledgements

This work was financially supported by the National Key Basic Research Program of China under contract No. 2007CB925002 and the National Nature Science Foundation of China under contract No. 10774146, 10774147, 50672099, 50701042 and Director's Fund of Hefei Institutes of Physical Science, Chinese Academy of Sciences.

References

[1] W.A. Yager, J.K. Galt, F.R. Merritt, Phys. Rev. 99 (1955) 1203–1210.
[2] U. Ghazanfar, S.A. Siddiqi, G. Abbas, Mater. Sci. Eng. B 118 (2005) 132–134.
[3] A.K.M. Akther Hossain, S.T. Mahmud, M. Seki, T. Kawai, H. Tabata, J. Magn. Magn. Mater. 312 (2007) 210–219.
[4] M. Ajmal, A. Maqsood, Mater. Sci. Eng. B 139 (2007) 164–170.
[5] S. Hashi, N. Takada, K. Nishimura, O. Sakurada, S. Yanase, Y. Okazaki, M. Inoue, IEEE Trans. Magn. 41 (2005) 3487–3489.
[6] H.L. Glass, Proc. IEEE 76 (1988) 151–158.
[7] J.H. Gao, Y.T. Cui, Z. Yang, Mater. Sci. Eng. B 110 (2004) 111–114.
[8] P.C. Dorsey, B.J. Rappoli, K.S. Grabowski, P. Lubitz, D.B. Chrisey, J.S. Horwitz, J. Appl. Phys. 81 (1997) 6884–6891.
[9] N. Matsushita, C.P. Chong, T. Mizutani, M. Abe, IEEE Trans. Magn. 38 (2002) 3156–3158.
[10] H.E. Zhang, B.F. Zhang, G.F. Wang, X.H. Dong, Y. Gao, J. Magn. Magn. Mater. 312 (2007) 126–130.
[11] Z.F. Zi, Y.P. Sun, X.B. Zhu, Z.R. Yang, J.M. Dai, W.H. Song, J. Magn. Magn. Mater. 320 (2008) 2746–2751.
[12] R. Krishnan, J. Appl. Phys. 39 (1968) 1340–1342.
[13] G. Herzer, Scr. Metall. Mater. 33 (1995) 1741–1756.
[14] Z.F. Zi, Y.P. Sun, X.B. Zhu, Z.R. Yang, J.M. Dai, W.H. Song, J. Magn. Magn. Mater. 321 (2009) 1251–1255.
[15] D. Yang, L.K. Lavoie, Y. Zhang, Z. Zhang, S. Ge, J. Appl. Phys. 93 (2003) 7492–7494.
[16] J.H. Liu, L. Wang, F. Li, J. Mater. Sci. 40 (2005) 2573–2575.